*Solid-State Electronics* Vol. 32, No. 12, pp. 1289–1295, 1989
Printed in Great Britain. All rights reserved

0038-1101/89 $3.00 + 0.00
Copyright © 1989 Pergamon Press plc

# NONEQUILIBRIUM ELECTRON DYNAMICS IN BIPOLAR TRANSISTORS

A. F. J. Levi, R. N. Nottenburg, Y. K. Chen, P. H. Beton,* and
M. B. Panish

AT&T Bell Laboratories, Murray Hill, New Jersey
07974-2070, USA
*Permanent address: Physics Department, University of Nottingham,
England, United Kingdom

## ABSTRACT

Experiments and calculations are used to illustrate the role of nonequilibrium electron transport in determining the performance of $InP/In_{0.53}Ga_{0.47}As$ heterostructure bipolar transistors. The intrinsic small signal response of devices operated under low voltage bias conditions is subpicosecond. However, with increasing bias the intrinsic speed of devices decreases because of scattering into low velocity subsidiary X- and L-valleys.

## KEYWORDS

Nonequilibrium electron transport; heterostructure bipolar transistors; intrinsic transit time; Monte Carlo.

## INTRODUCTION

The intrinsic small signal current gain cutoff frequency, $f_T$, of a bipolar transistor is given by the emitter-collector delay time

$$\tau_{ec}^{o} = 1/2\pi f_T = r_e(C_e + C_c) + \tau_b + \tau_c \,, \tag{1}$$

where $C_e$ is the emitter capacitance, $C_c$ is the collector capacitance, $\tau_b$ is the transit time across the base of thickness $Z_b$, $\tau_c$ is the transit time across the collector space charge region of thickness $Z_c$, and $r_e$ is the dynamic emitter resistance. In the expression for $\tau_{ec}^{o}$ we ignore parasitic delays due to emitter and collector series resistance which are extrinsic to the basic physics of device operation. A transistor making use of high velocity nonequilibrium electron transport should be a fast device because of $\tau_b$ and $\tau_c$ will be relatively small. However, since the term $r_e(C_e + C_c)$ in Eqn. 1 is current dependent via the dynamic emitter resistance $r_e = n\, k_B T/I_e$ (where $I_e$ is the emitter current and n is the junction ideality factor), it is also important to operate such a transistor at a high current density. The transistor's maximum frequency of oscillation, $f_{max}$, is related to $f_T$ via the expression

$$f_{max} \simeq (f_T/8\pi R_b C_c)^{1/2}, \tag{2}$$

where $R_b$ is the base resistance. Obviously, for high $f_{max}$ a low $R_b$ is advantageous.

All the above requirements can be met in a suitably designed heterostructure bipolar transistor (HBT). In Fig. 1 we show a schematic diagram of a device with an abrupt wide band gap emitter which injects conduction electrons with excess kinetic energy E and angular spread $<\theta> \simeq \tan^{-1}(k_B T/E)^{1/2}$ into a narrow band gap degenerately doped p-type base. Low base resistance, $R_b$, can be achieved using very heavy base doping levels in the range $p = 10^{20}$ $cm^{-3}$ (Hamm and co-workers, 1989). High impurity concentrations such as these do not significantly increase $\tau_b$ since nonequilibrium electron transport in the base is largely unaffected (Levi, 1988).

The role of nonequilibrium electron transport in determining the performance of N-p-n HBTs has been explored experimentally using static measurement techniques. Hot electron spectroscopy has been used to show that extreme nonequilibrium electron transport is possible in both the base and collector space charge region (Berthold and co-workers, 1988 and 1989). The experiments show that when $Z_b$ and $Z_c$ approach the electron mean free path $\lambda$, of the injected charge carriers, a significant number of electrons traverse the active region of the device without scattering. The results suggest that with proper transistor design, very fast HBTs which make use of the high velocities ($\sim 10^8$ $cms^{-1}$) associated with extreme nonequilibrium electron transport should be possible. Such transport has also

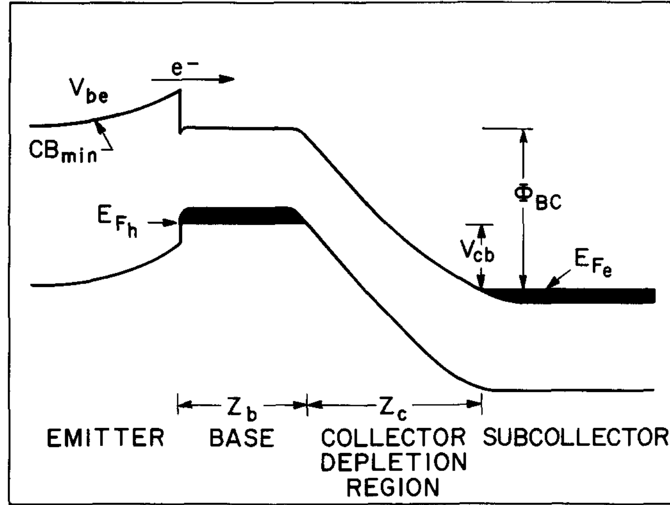


Fig. 1. Schematic band diagram of a HBT under bias. A wide band gap emitter injects electrons into states with excess kinetic energy E in the base region. The base and collector are of thickness $Z_b$ and $Z_c$ respectively. The collector-base bias is $V_{cb}$ and the total potential drop in the collector is $\Phi_{bc}$. The conduction band minimum, $CB_{min}$, the hole Fermi energy, $E_{F_h}$, and the electron Fermi energy, $E_{F_e}$, are indicated.

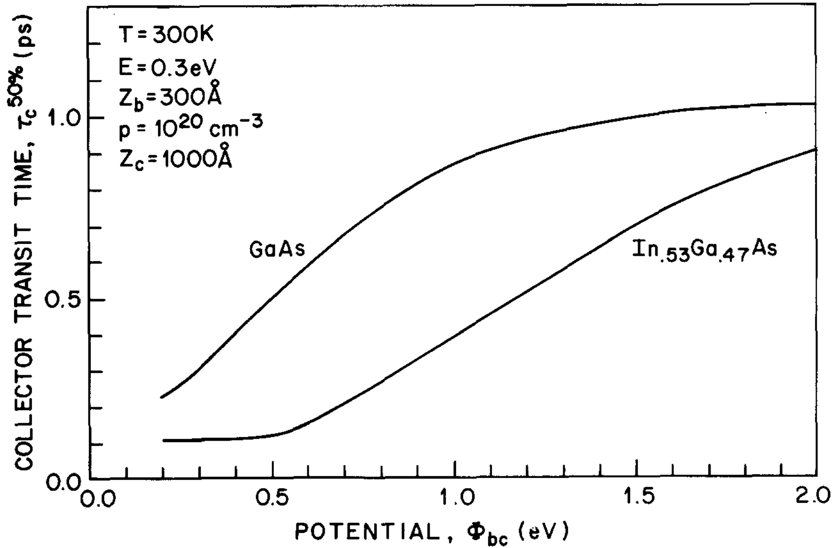


Fig. 2. Calculated collector transit time, $\tau_c^{50\%}$, in GaAs and $In_{0.53}Ga_{0.47}As$ as a function of base/collector potentials, $\Phi_{bc}$, for E = 300 meV, $Z_b$ = 250Å, p = $1 \times 10^{20}$ $cm^{-3}$, $Z_c$ = 1000Å, and T = 300K.

been shown to improve the static current gain of HBTs (Levi and co-workers, 1989; Jalali and co-workers, 1989). In a transistor utilizing diffusive charge transport in the base, recombination processes can reduce current gain in structures with small emitter stripe dimension, W. Recombination can take place on the exposed base adjacent to the emitter stripe and in the extrinsic bulk base region. For small W, this results in a reduction in current gain. However, for a transistor in which extreme nonequilibrium base transport is significant there is a decrease in the non-radiative interaction volume of around $\Delta_v = (e\, Z_b\, v^{diffusive}/4\mu E)^{1/2}$, where $\mu$ is the mobility of minority carriers in the base of a diffusive transistor and $v^{diffusive}$ is the diffusion velocity. Typically this translates into a factor of approximately three improvement in current gain for small W. An additional increase in current gain can arise from a reduced cross section for non radiative processes due to the relatively large electron velocity in a transistor which uses nonequilibrium base transport.

Another advantage of charge carriers which move with a high average velocity, v, is increased current density of operation. High current density is important for high speed because of the associated reduction of emitter charging time. A large velocity, v, also increases the space charge limited collector current density $j = n e v$, where n is the impurity concentration in the collector space charge region.

## DYNAMIC RESPONSE

While it is clear from the above that much has been learnt from static electrical measurements it is interesting to consider the dynamic response of HBTs which make use of nonequilibrium electron transport. Numerical simulations show that collector transit time, $\tau_c$, is an important delay in devices of the type shown schematically in Fig. 1. In Fig. 2 we present results of calculating the room temperature impulse response delay for 50% of electrons to traverse a collector with $Z_c = 1000$Å as a function of potential, $\Phi_{bc}$. As may be seen, a GaAs HBT operated near $V_{cb} = 0$ V (i.e. $\Phi_{bc} \simeq 1.5$ eV) has $\tau_c^{50\%} \simeq 1$ ps and $v^{50\%} \simeq 10^7$ cms$^{-1}$. Under these operating conditions, transport is controlled by equilibrium drift-diffusive processes and GaAs has no performance advantage over Si. In contrast, an $In_{0.53}Ga_{0.47}As$ HBT operated near $V_{cb} = 0$ V (i.e. $\Phi_{bc} \simeq 0.75$ eV) has a considerably smaller $\tau_c^{50\%} \simeq 0.25$ ps and a factor of four greater average velocity $v^{50\%} \simeq 4 \times 10^7$ cms$^{-1}$. Naturally, HBTs fabricated from $In_{0.53}Ga_{0.47}As$ show significant high frequency performance advantages over both GaAs and Si (Nottenburg and co-workers, 1989; Chen and co-workers, 1989).

Using devices similar to those reported by Chen and co-workers (1989) we have performed experiments which measure intrinsic transit time effects. The transistors have an n-type InP emitter with area $3 \times 11$ $\mu m^2$, the 500Å thick base is p-type $In_{0.53}Ga_{0.47}As$ doped to $1 \times 10^{20}$ cm$^{-3}$, the 3000Å thick collector space charge region is doped n-type to $3 \times 10^{16}$ cm$^{-3}$, and the subcollector is heavily doped n-type. Microwave measurements were performed in the 1 GHz to 40 GHz range with the sample maintained at a temperature of T = 80K. This low operating temperature ensured that the intrinsic transit time is the dominant transistor delay and parasitics such as emitter charging time are relatively small. Typical results of measuring small signal current gain $|h_{21}|$ with frequency are given in Fig. 3. The broken curve shows $f_T = 244$ GHz extrapolated using a $-20$ dB/decade roll-off.

For $\Phi_{bc} > 0.85$ eV, the collector space charge region is fully depleted, $Z_c$ is constant, and any change in transit delay $\tau_F = \tau_b + \tau_c$ with $\Phi_{bc}$ is due to transport processes intrinsic to the device. It is clear from Fig. 4 that the measured $\tau_F$ increases by a factor of about two from 0.32 ps at $\Phi_{bc} = 0.88$ eV to 0.63 ps at $\Phi_{bc} = 1.6$ eV. To understand the origin of this effect we have used Monte Carlo techniques to simulate nonequilibrium electron transport in these devices. The calculations are performed assuming a semiclassical description of device operation is valid. Thus, electron motion is modeled using local trajectories and the influence of quantum mechanical reflections from the conduction band profile is ignored. Scattering mechanisms in the base include screened ionized impurity and majority carrier/optical phonon excitations. The dominant scattering processes in the collector are due to optical phonons and intervalley transfer. The methods used to calculate these scattering rates have been described previously (Combescot and Noziers, 1972; Levi and Yafet, 1987; Bardyszewski and Yevick, 1989; Beton and Levi, 1989; Massengill and co-workers, 1986). The numerical techniques used in the simulation are similar to those of Beton and Levi (1989) and the parameters for $In_{0.53}Ga_{0.47}As$ were taken from Massengill and co-workers (1986).

The broken curve in Fig. 5 shows the calculated collector current due to a unformly injected 3.6 ps emitter current pulse (solid curve) of 24,000 electrons for $\Phi_{bc} = 1$ eV. The large signal impulse response in Fig. 5 cannot be described in terms of a single transit delay time. The underlying reason for this may be seen by examining Fig. 6 in which

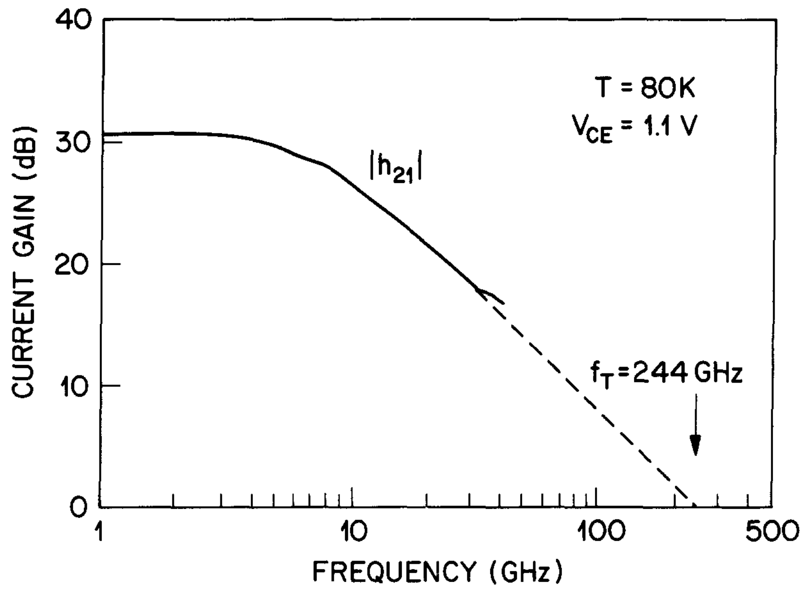


Fig. 3. The solid curve shows the measured small signal common emitter current gain $|h_{21}|$ with frequency, f, in the range 1 to 40 GHz. The transistor has an emitter area of $3 \times 11\ \mu m^2$ with a collector current $I_c = 31$ mA and collector-to-emitter bias $V_{ce} = 1.1$V. The broken curve shows a $-20$ dB/decade roll-off extrapolating to a cutoff frequency $f_T = 244$ GHz. Measurements were performed with a sample maintained at a temperature of T = 80K.

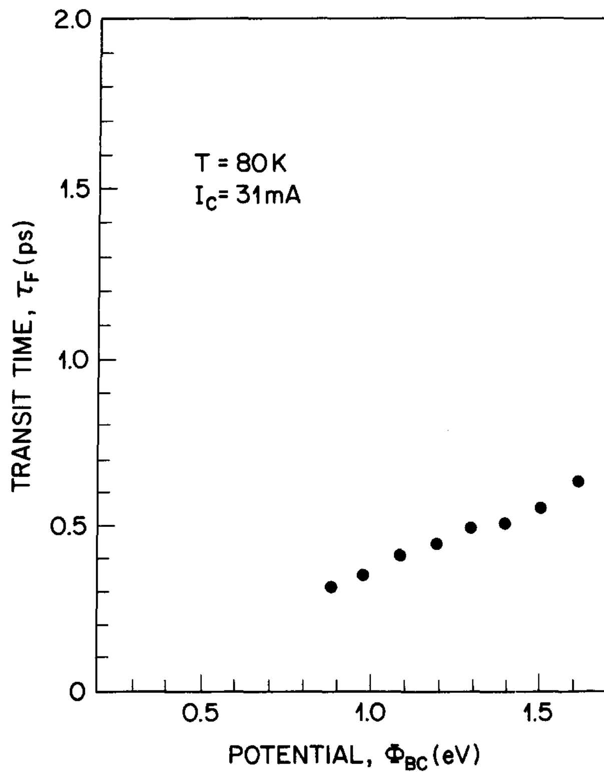


Fig. 4. Measured transit delay $\tau_F$ as a function of $\Phi_{bc}$.

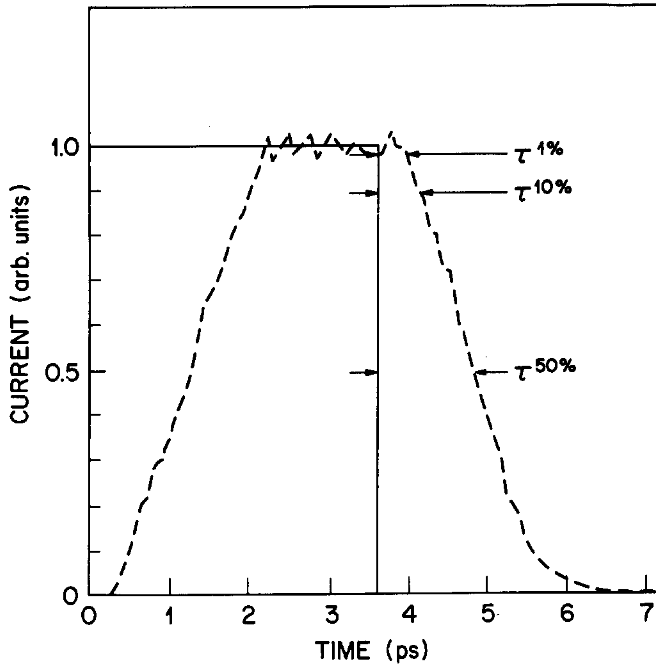


Fig. 5. Numerically simulated $In_{0.53}Ga_{0.4}As$ collector current response (broken line) to a uniformly injected 3.6 ps emitter current pulse (solid line) containing 24,000 electrons with $\Phi_{bc} = 1.0$ eV. Parameters used in calculation were $E = 300$ meV, $Z_b = 500$Å, $Z_c = 3000$Å, $p = 1 \times 10^{20}$ cm$^{-3}$, and $T = 80$K.

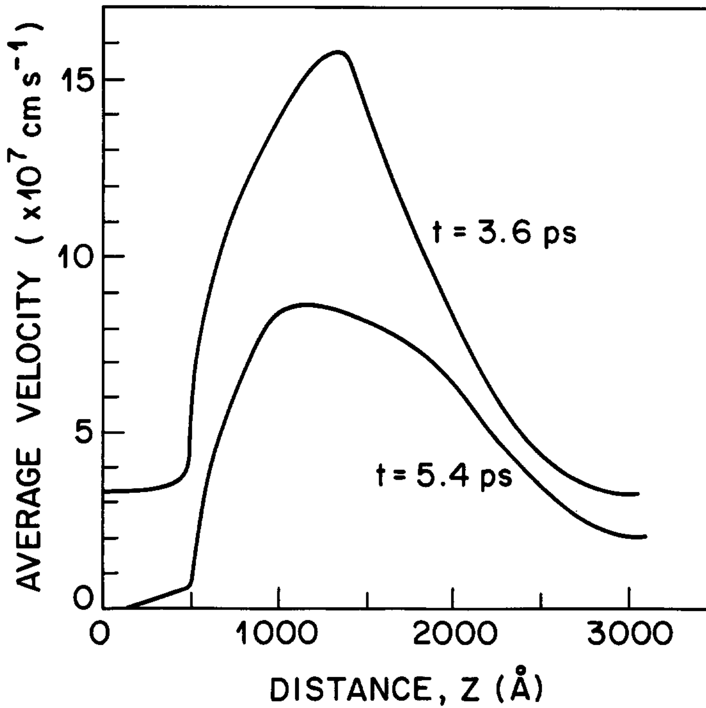


Fig. 6. Calculated average electron velocity as a function of distance, Z from the emitter/base junction for the parameters used in Fig. 5.

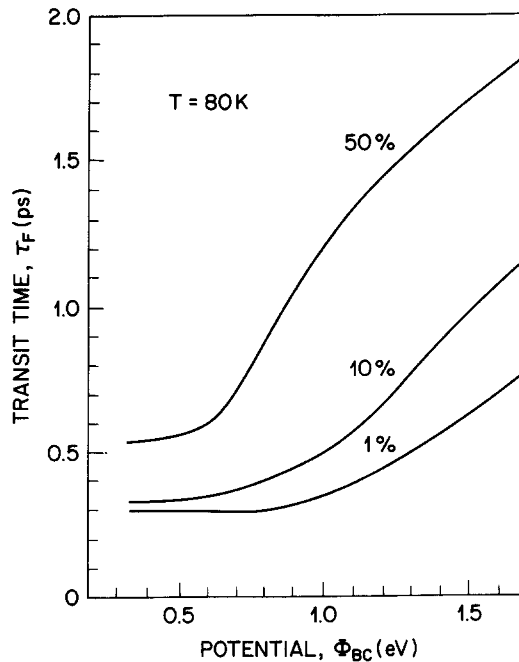


Fig. 7. Results of calculating $\tau_F^{1\%}$, $\tau_F^{10\%}$ and $\tau_F^{50\%}$ as a function of $\Phi_{bc}$ for the parameters used in Fig. 5.

average electron velocity is plotted at time t = 3.6 ps and t = 5.4 ps for $\Phi_{bc}$ = 1 eV as a function of distance, Z, from the emitter/base junction. As the transistor switches from the on (t = 3.6 ps) to the off (t = 5.4 ps) state high velocity central Γ-valley electrons rapidly sweep out of the base region ($0 < Z < 500$Å). However, electrons accelerated in the large electric field in the collector space charge region can gain enough kinetic energy to scatter into the low velocity subsidiary L- and X-valleys located 0.55 eV and 1.15 eV above the conduction band minimum respectively. These low velocity electrons take a longer time to transit the device and account for the tail in the large signal, $\tau_F^{50\%}$ temporal response shown in Fig. 5. On the other hand, $\tau_F^{1\%}$ is dominated by the fastest Γ-valley electrons.

In Fig. 7 we plot results of calculating $\tau_F$ for 1%, 10% and 50% signal delay as a function of $\Phi_{bc}$. The agreement between the calculated $\tau_F^{1\%}$ and the experimental data in Fig. 4 is not too bad suggesting that the measured increase in small signal $\tau_F$ with increasing $\Phi_{bc}$ is due to intervalley scattering.

## CONCLUDING REMARKS

The fastest bipolar transistors make use of high velocity Γ-valley nonequilibrium electron transport in $In_{0.53}Ga_{0.47}As$. The experimentally observed increase in intrinsic transit delay with increasing $\Phi_{bc}$ is confirmed by semiclassical calculations and is due to scattering into low velocity subsidiary valleys in the collector. Calculations indicate that for a thin highly doped base ($p > 10^{20}cm^{-3}$ ) the transit time, $\tau_b$, is negligible and the collector transit time, $\tau_c$, dominates the intrinsic transistor response. An important consequence of this is that ultra high speed HBTs perform best under small signal and low collector voltage bias conditions. Optimum collector bias is chosen so as not to significantly populate low velocity subsidiary minima in the semiconductor.

With the further reduction in $Z_b$ and $Z_c$ it is expected that substantial coherent electron transport between emitter and subcollector can occur. In this situation semiclassical calculations, such as those discussed above, inadequately describe transistor operation and an alternative, quantum mechanical, description will have to be found. As an example, quantum interference effects are important when significant changes in electron velocity occur on the scale of the particle wavelength and it has been pointed out by Gelfand and co-workers (1989) that in this situation inelastic scattering can influence elastic scattering (quantum mechanical reflection and transmission).

REFERENCES

Bardyszewski, K., and Yevick, D. (1989). *Appl. Phys. Lett. 54*, 837.
Berthold, K., Levi, A. F. J., Walker, J., and Malik, R. J. (1988). *Appl. Phys. Lett. 52*, 2247.
Berthold, K., Levi, A. F. J., Walker, J., and Malik, R. J. (1989). *Appl. Phys. Lett. 54*, 813.
Beton, P., and Levi, A. F. J. (1989). *Appl. Phys. Lett. 55*, 250.
Chen, Y. K., Nottenburg, R. N., Panish, M. B., Hamm, R. A., and Humphrey, D. A. (1989). *IEEE Electron Device Lett. EDL-10*, 267.
Combescot, M., and Noziers, P. (1972). *Solid State Comm., 10*, 301.
Gelfand, B. Y., Schmitt-Rink, S., and Levi, A. F. J. (1989). *Phys. Rev. Lett. 62*, 1683.
Hamm, R. A., Panish, M. B., Nottenburg, R. N., Chen, Y. K., and Humphrey, D. A. (1989). *Appl. Phys. Lett. 54*, 2586.
Jalali, B., Nottenburg, R. N., Chen, Y. K., Levi, A. F. J., Sirco, D., Cho, A. Y., and Humphrey, D. A. (1989). *Appl. Phys. Lett. 54*, 2333.
Levi, A. F. J., and Yafet, Y. (1987). *Appl. Phys. Lett. 51*, 42.
Levi, A. F. J. (1988). *Electron. Lett. 24*, 173.
Levi, A. F. J., Nottenburg, R. N., Chen, Y. K., and Cunningham, J. E. (1989). *Appl. Phys. Lett. 54*, 2250.
Massengill, L. W., Glisson, T. H., Hauser, J. R., and Littlejohn, M. A. (1986). *Solid State Electron 29*, 725.
Nottenburg, R. N., Chen, Y. K., Panish, M. B., Humphrey, D. A., and Hamm, R. A. (1989). *IEEE Electron Dev. Lett. EDL-10*, 30.